Solid Freeform Fabrication 2018: Proceedings of the 29th Annual International Solid Freeform Fabrication Symposium – An Additive Manufacturing Conference
Reviewed Paper

EXAMINATION OF THE CONNECTION BETWEEN SELECTIVE LASER-MELTED COMPONENTS MADE OF 316L STEEL POWDER ON CONVENTIONALLY FABRICATED BASE BODIES

Martin Link[1], Tobias Haefele[1], Eberhard Abele[1]

[1] Institute of Production Management, Technology, and Machine Tools (PTW),
Technische Universität Darmstadt, Darmstadt, Germany

Abstract

The advantages of selective laser melting lie in the production of complex, small components in small batches. For large-volume components, the use of additive manufacturing (AM) processes is limited by the available installation space, low build rates, and high material costs. For the production of large and less complex workpieces, conventional manufacturing processes such as milling are more economical. The background of this study was to combine both processes to decrease manufacturing times. For this purpose, a body made of 316L (1.4404) steel powder was printed using selective laser melting on conventionally manufactured stainless-steel base bodies. The use of multi-materials enables optimized machinability in the respective manufacturing process. This paper examines the hardness properties of multi-material samples and uses micrographs to analyze the microstructure of their connection area. A complete connection between hybrid components made of comparable materials was determined.

1. Introduction

Additive manufacturing (AM), an emerging field in manufacturing technologies, features the principle of building solid parts directly from 3D-CAD data by the layer-by-layer addition of materials, which may be plastic, metal, concrete, or, as expected in the future, human tissue. According to Wohler's Report, 135 manufacturers produced AM systems in 2017 compared to 65 manufacturers in 2015. Today, established manufacturers are under pressure due to the huge number of new machines and unprecedented levels of competition in the additive production marketplace. In 2017, the AM segment of worldwide sales are increased by 20.9% to US $7.336 billion [1]. Powder-bed-fusion-based AM processes use thermal energy to selectively fuse regions of a powder bed [2]. This study focuses on the laser melting of metal powders, often also referred to as selective laser melting (SLM). Given the current state of the art, low construction rates and high material costs limit the economics of the SLM process for large-volume components [3]. In this study, the relationship between an additively built volume and a conventionally manufactured base body was investigated. The advantages of the SLM process lie in the production of complex components in small batches. Due to their high rates of cooling, the components achieve increased strength values compared to those of cast components [4]. Conventional manufacturing processes, in contrast, are better suited for large quantities and less complex components. By combining additive construction using the SLM process with conventionally manufactured base bodies, the advantages of both processes can be obtained. In this paper, this combination of processes is referred to as a hybrid process. This hybrid process is already being used in industry. For example, large components are being produced by fine forging a base body and then using SLM to add complex structures. To be able to produce hybrid components for industrial use, multiple factors must be considered. The base bodies must have a flat surface of low surface roughness, which is fixed parallel to the powder bed. In the hybrid production of components, the connection between the two materials is of particular concern and must be examined in detail. In this regard, a material combination must be selected that enables effective hybrid production. Furthermore, the first powder layer must be of a defined height to enable process reproducibility. Tensile tests of hybrid specimens show that the tensile rods fail not in the material transition but in the weaker area of the two materials [5–7]. Furthermore, hybrid samples with different aspect ratios (1:2, 1:1, 2:1) of the hybrid samples were examined, which also showed no influence on the tensile strength [8]. Another aspect for consideration is surface roughness, which is a decisive factor in many applications. The fatigue performance of AM parts is primarily dependent on their surface roughness [9, 10]. To meet the requirements of hybrid components, the additive volume must be post processed, e.g., grinded, shot-peened, or machined.

This paper investigates the connection between the base body and the additively applied volume. To do so, structural and hardness investigations were conducted in the connection area to identify critical factors in the industrial production of components in this area of investigation.

2. Research methodology

The experiments were conducted using a commercially available SLM system EOS M290 from EOS GmbH (Germany), which uses a 400 W Yb fiber laser focused on a 100-µm spot. In all the experiments in this study, a gas atomized stainless steel 316L powder with a particle distribution range of 11 µm to 54 µm and a d50 of 25 µm was used. The 316L_SurfaceM291 parameter set qualified by the machine manufacturer was used for the additive build-up and the layer thickness was set to 20 µm. The conventionally manufactured base bodies consist of 1.4301 stainless steel. Tables 1 and 2 list the chemical compositions of the 1.4301 and 1.4404 steel materials.

Table 1: Chemical composition of the 1.4404 steel material [11]

Element	Fe	Cr	Ni	Mo	C	Mn	Cu	P	S	Si	N
Min.	Balance	17.00	13.00	2.25	-	-	-	-	-	-	-
Max.		19.00	15.00	3.00	0.03	2.00	0.50	0.025	0.01	0.75	0.1

Table 2: Chemical composition of the 1.4301 steel material [12]

Element	Fe	Cr	Ni	C	Mn	P	S	Si	N
Min.	Balance	17.50	8.00	-	-	-	-	-	-
Max.		19.50	10.50	0.07	2.00	0.045	0.015	1.00	0.11

The 252 mm × 252 mm × 20-mm substrate plate has a grid of through holes. The base-body measures 10 mm × 10 mm × 25 mm and has 13-mm deep M4 threaded holes. The additively built body measures 9 mm × 9 mm × 10 mm. 20 base bodies were fixed to the substrate plate with Allen screws (Figure 1).

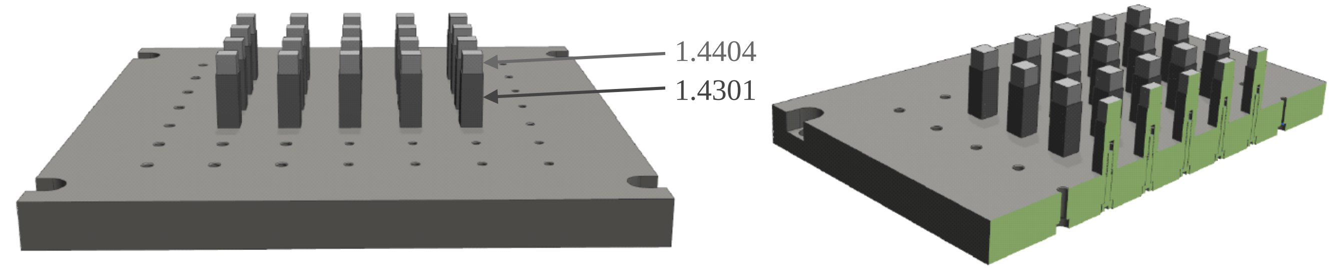

Figure 1: Schematic illustration of the hybrid samples on the substrate plate with base bodies of 1.4301 and additive built-up volumes of 1.4404

The surface plane of the base bodies is ground to ensure a homogeneous roughness profile and a parallel plane between the specimens and the building platform. After the building process, the components were cleaned in an ultrasonic bath and the samples embedded with Struers EpoFix and EpoFix hardener (ratio 25:3), which then hardened for 15 hours. The surfaces of the hybrid specimens to be examined are ground in stages using 180-, 320-, 500-, 1000-, 2500- and 4000-grit abrasive paper. In the final polishing process, a surface roughness of Rz 1 µm was achieved. Hardness tests were performed with Struers' DuroScan20 semi-automatic hardness testing system and Vickers low-load and microhardness tests.The indenter used in Vickers hardness measurement consists of a square diamond pyramid with a square base whose sides are inclined 136° to each other. Due to the proportionality of the test load to the indentation surface, Vickers hardness values are load-dependent. For particularly low loads, however, properties of the material, e.g., its surface tension, have an effect on the test load. For this reason, in addition to the microhardness tests, test loads with low-load hardness were performed for comparison. 15 HV0.05 measuring points were used for microhardness measurement and three measuring points in the connection area for low-load hardness measurement. The Vickers hardness (HV) values are calculated by (Eq.1), as follows:

$$HV = \frac{(0{,}102 * F)}{A} = \left(\frac{2 * \sin(68°)}{d}\right) * 0{,}102 * F \qquad \text{(Eq.1)}$$

where F is the test force, A is the area, and d is the mean value of the diagonals. The holding time is 7 seconds [13]. To make the structures of the hybrid samples visible, immersion etching was performed in a Behara 2 color etching mixture. This is a precipitation estimation in which the cut surface reacts with the etchant, whereby the thickness and color of the precipitation layer is influenced by the crystal orientation and phase structure of the material. To obtain an overview of the structure, an optical microscope LEICA DM6000 was used for the examinations. To analyze the heat-affected zone, we used energy dispersive X-ray spectroscopy.With a scanning electron microscope from Phenom-World BV 15 measurements were performed at a distance of 100 µm from the edge of the hybrid part. The acceleration voltage used was 15 kV.To investigate the heat-affected zone, a single powder layer was additively built up and examined on additional samples.

3. Results

The macroscopic examination of the hybrid samples revealed no cracks or discoloration of the material in the connection area.The surface roughnesses of the two areas were quite different, as shown in the inset of Figure 2.

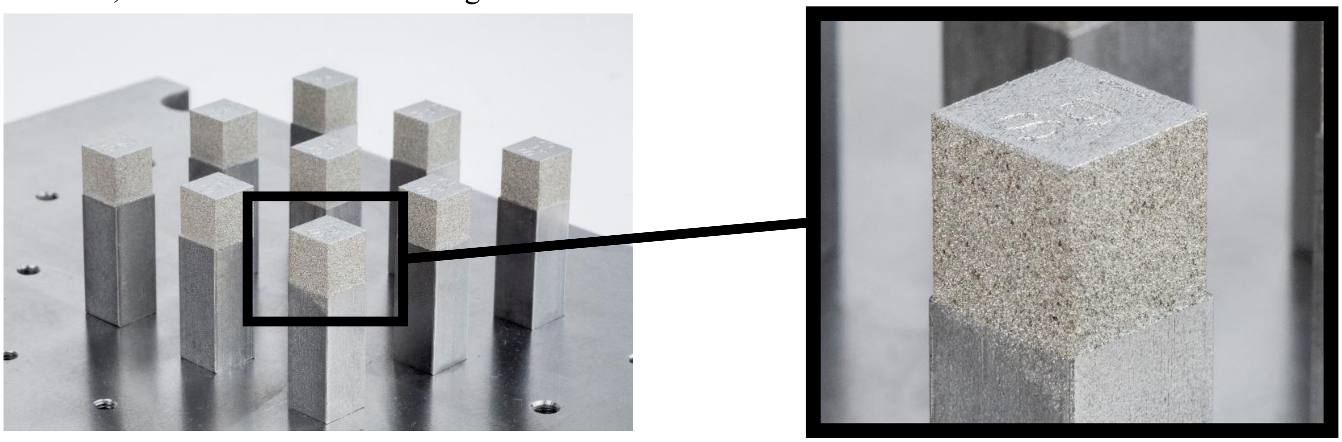

Figure 2: Produced hybrid samples on the substrate plate

The investigations with optical and scanning electron microscopes showed neither cracks nor larger visible porosities in the connection area of the hybrid samples. This connection is characterized by melting traces from the laser radiation. The widths and depths of the melt tracks vary. The area of the base body 1.4301 shows strong line-shaped inclusions of manganese sulfide, which formed during the production of the raw material. The structure of the additive area is very different from that of a conventionally cast structure (Figure 3).

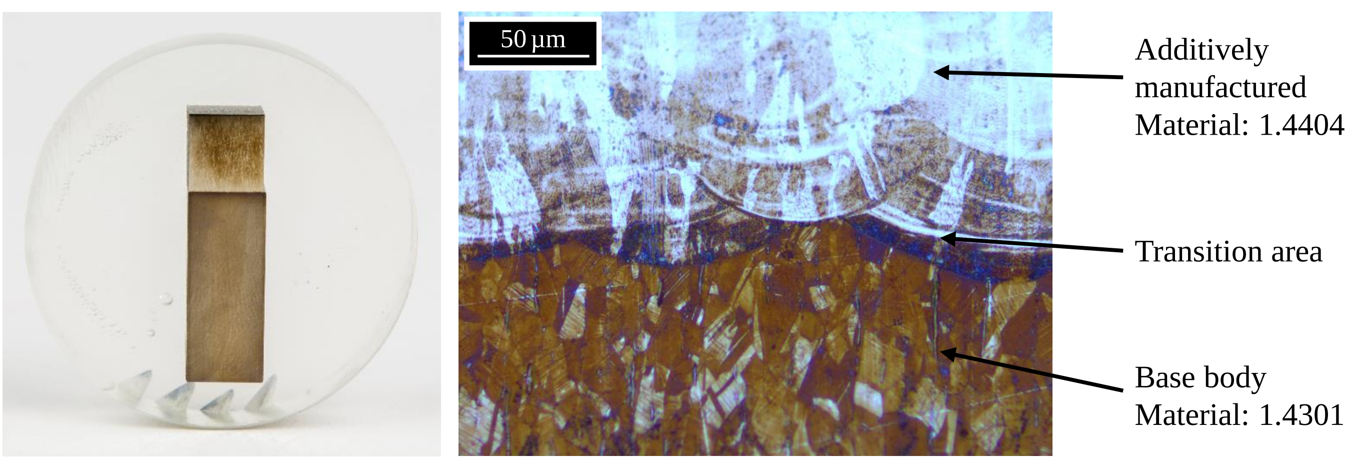

Figure 3: Micrograph of hybrid sample; macroscopic (left) and microscopic (right)

In the connection area above the base body, material mixing is evident. This area is followed by a heat-affected zone in the base-body area, which shows a typical austenitic structure. The structure of the base body shows row-shaped delta-ferrite fractions. Compared to the heat-affected zone, the base body has a high proportion of deformation-induced martensite. Viewed from the edge, the heat-affected zone increases from 40 µm to 130 µm inside the component. This behavior can also be seen in the test series, in which only one layer of powder is melted onto the base body (Figure 4).

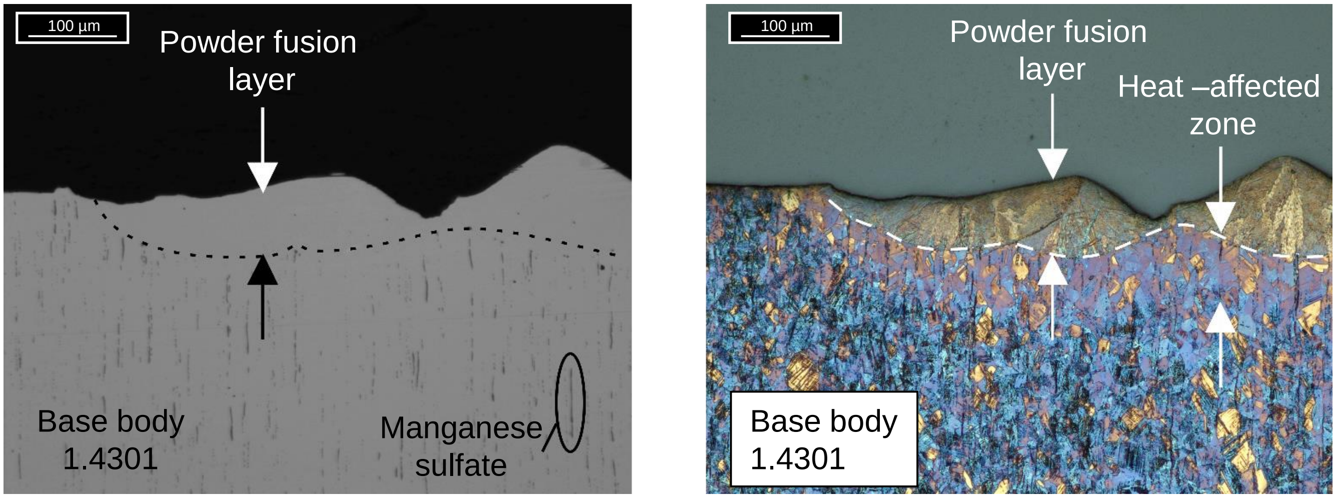

Figure 4: Polished (left) and etched (right) sample after exposure of one powder layer

The results of the microhardness tests show a hardness of 215 ± 3 HV0.05 in the additive range, which corresponds to a low load hardness value.

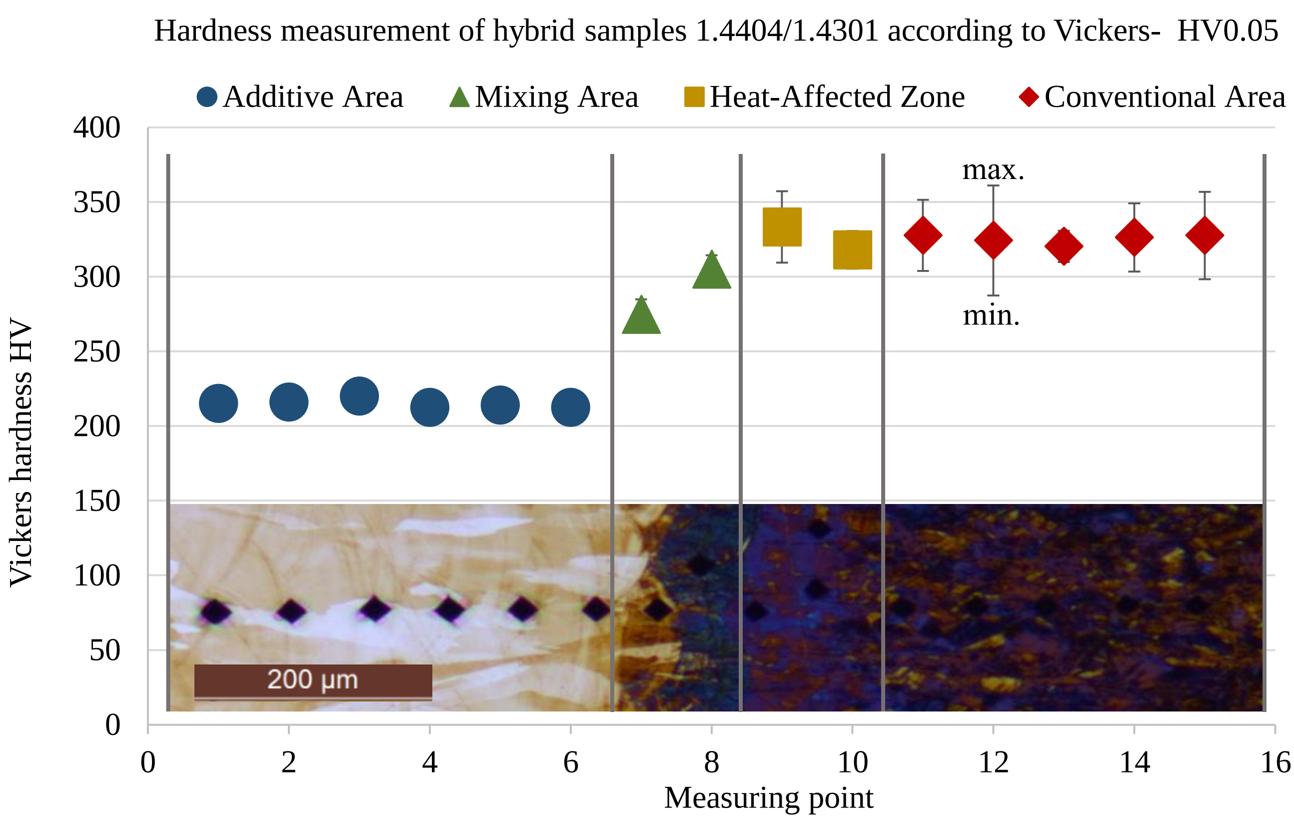

Figure 5: Vickers hardness measurement HV0.05 of the hybrid sample

In the area of material mixing, the hardness values gradually increase and at the end of this zone they are within the hardness range of the 1.4301 material. Hardness values of 320 ± 8 HV0.05 can be seen both in the heat-affected zone and in the conventional area (Figure 5).

4. Discussion

The investigations using optical and scanning electron microscopes indicate that a complete connection of the two materials was achieved, since no cracks and only a very small degree of porosity are evident. This confirms the results of previous tests on tensile specimens [8]. The different widths and depths of the melt tracks are due to the different orientations of the exposure scan vectors, which differ for each layer.

The difference in the microstructures of the additive and conventionally produced volumes is due to the layered structure. Due to the laser exposure it can be assumed that the microstructure is oriented in the direction of the highest temperature gradient. [14]. The layered exposures remelt the solidified material and, depending on the orientation of the scan vector, lead to an uneven orientation of the melt traces.

The material mixing in the connection area can be explained by the dynamics of the melt pool. During the exposure of the first powder layer, the base body absorbs part of the laser radiation, melting it and releasing components of the 1.4301 material. Due to the dynamic of the melt pool, the melt of the build-up body mixes with those of the base body [15]. The optical microscopic investigations suggest that with each new exposure the alloy components of the underlying layer mix with the top layer and are carried upwards. The degree of this material mixing is reduced with each new layer of material applied.

In the base body, microstructural changes in the connection area and heat-affected zone are evident. Since deposits of deformation-induced martensite form in the untreated state of the 1.4301 base material, the heat-affected zone can be identified by the area free of deformation-induced martensite, which is converted to austenite by the temperature effect of the build-up process.Compared to multi-layer exposure, the depth of the heat-affected zone is significantly lower with a single melted layer due to the lower heat input. The increased hardness in the connection area can be explained by the mixing of the two materials, wherein an inhomogeneous material distribution occurs [7]. Despite the changed microstructure, the lack of deformation-induced martensite does not affect the hardness of the heat-affected zone. It can be assumed that precipitation hardening leads to a compensation hardness in this area. Thus, laser processing results in changed hardness values only in the area of material mixing.

5. Summary and outlook

In this work, the connection of hybrid components using different materials was investigated. 1.4404 steel material was used for the additively manufactured body and 1.4301 steel for the conventionally manufactured base body. The samples were examined by optical microscopy, scanning electron microscopy and hardness measurement. The following conclusions can be drawn from the results:

- A complete connection was made between hybrid components of comparable materials. No cracks or relevant pores were found.

- The connection area of the hybrid samples can be divided into the four zones: purely additive, material mixing, heat-affected, and conventional areas. The material mixing occurs in response to the dynamics of the melt pool.

During the design and execution of the tests it was determined that both materials must be compatible in order to ensure a crack and pore-free connection. Furthermore, the connecting surface on the base body must have low roughness and be parallel with the coating plane. In addition, exact positioning on the base plate and a strictly defined height of the first powder layer are required. Future research will focus on which material combinations prove most effective in the production of hybrid samples. Notched bar impact tests should be conducted to enable greater understanding of the mechanical behavior of hybrid components.

Acknowledgments

This work was funded by the Federal Ministry of Education and Research (funding code 02P16K021). The authors are grateful for this support.

References

[1] Wohlers T (2018) Wohlers Report: 3d printing and additive manufacturing state of the industry. Wohlers Associates, Fort Collins

[2] ASTM F2792-12a (2012) Terminology for Additive Manufacturing Technologies, West Conshohocken, PA

[3] VDMA - Arbeitsgemeinschaft Additive Manufacturing (2017) Technology Scout 2017: Technologien, Anwendung und Hersteller, Frankfurt

[4] BARTOLOMEU F, Bucuimeanu M, PINTO E et al. (2017) 316L stainless steel mechanical and tribological behavior—A comparison between selective laser melting, hot pressing and conventional casting. Additive Manufacturing 16: 81–89. doi: 10.1016/j.addma.2017.05.007

[5] Demir AG, Previtali B (2017) Multi-material selective laser melting of Fe/Al-12Si components. Manufacturing Letters 11: 8–11. doi: 10.1016/j.mfglet.2017.01.002

[6] Liu Q, Wang Y, Zheng H et al. (2016) Microstructure and mechanical properties of LMD–SLM hybrid forming Ti6Al4V alloy. Materials Science and Engineering: A 660: 24–33. doi: 10.1016/j.msea.2016.02.069

[7] Sing SL, Lam LP, Zhang DQ et al. (2015) Interfacial characterization of SLM parts in multi-material processing: Intermetallic phase formation between AlSi10Mg and C18400 copper alloy. Materials Characterization 107: 220–227. doi: 10.1016/j.matchar.2015.07.007

[8] Sehrt JT (2010) Möglichkeiten und Grenzen bei der generativen Herstellung metallischer Bauteile durch das Strahlschmelzverfahren. Zugl.: Duisburg-Essen, Univ., Diss., 2010. Berichte aus der Fertigungstechnik. Shaker, Aachen

[9] Greitemeier D, Dalle Donne C, Syassen F et al. (2015) Effect of surface roughness on fatigue performance of additive manufactured Ti–6Al–4V. Materials Science and Technology 32(7): 629–634. doi: 10.1179/1743284715Y.0000000053

[10] Stoffregen HA, Butterweck K, Abele E (2014) Fatigue Analysis in Selective Laser Melting: Review and Investigation of Thin-walled Actuator Housings. Bourell D (Hrsg) 25. Solid Freeform Fabrication Symposium

[11] EOS GmbH - Electro Optical Systems (2014) Material Data Sheet 316L. https://cdn0.scrvt.com/eos/ccaf69b7dbb3dc84/412597466f6c/EOS_StainleesSteel_316L.pdf

[12] ThyssenKrupp Materials International Material Data Sheet 1.4301. http://www.s-k-h.com/media/de/Service/Werkstoffblaetter_englisch/Edelstahlrohre/1.4301_engl.pdf. Accessed 26 Jun 2018

[13] Herrmann K, Polzin T, Kompatscher M et al. (2014) Härteprüfung an Metallen und Kunststoffen: Grundlagen und Überblick zu modernen Verfahren, expert-verlag, Renningen

[14] Srivatsan TS, Sudarshan TS (eds) (2016) Additive manufacturing: Innovations, advances, and applications. CRC Press, Boca Raton, Fla.

[15] Cloots M (2017) Empirische und simulative Studie über die Verarbeitbarkeit von IN738LC mittels SLM. ETH Zurich